University of Sistan and Baluchestan

Chemical Process Design

Available online at http://cpd.usb.ac.ir/



Design and Thermodynamic Evaluation of An Integrated RO-AGMD-Spray Dryer System for Solar-Powered Zero Liquid Discharged Desalination

Pouria Moradalizadeh[1], Taleb Zarei[2]✉, Ehsan Abedini[3], Jamshid khorshidi[4]

[1] Department of Mechanical Engineering, University of Hormozgan, Bandar Abbas, Iran. Email: P.moradalizadeh.phd@hormozgan.ac.ir
[2] Corresponding Author, Department of Mechanical Engineering, University of Hormozgan, Bandar Abbas, Iran. Email: talebzarei@hormozgan.ac.ir
[3] Department of Mechanical Engineering, University of Hormozgan, Bandar Abbas, Iran. Email: abedini@hormozgan.ac.ir
[4] Department of Mechanical Engineering, University of Hormozgan, Bandar Abbas, Iran. Email: khorshidi@hormozgan.ac.ir

ARTICLE INFO

Article type:
Research Article

Article history:
Received: 2026-07-13
Received in revised form: 2026-10-31
Accepted: 2026-11-02
Available online: 2026-11-02

Keywords: *Reverse osmosis (RO); Air gap membrane distillation (AGMD); Spray dryer; Zero liquid discharge (ZLD); Solar thermal energy*

ABSTRACT

This study presents a thermodynamic model of a solar-driven hybrid desalination system integrating reverse osmosis (RO), air gap membrane distillation (AGMD), and a spray dryer to achieve zero liquid discharge (ZLD) and enhance freshwater recovery. In this configuration, seawater is first treated by RO, producing freshwater and a concentrated brine stream that is further processed by AGMD using thermal energy supplied by a parabolic trough collector (PTC). The remaining brine is converted into solid salt via spray drying, eliminating liquid waste. A combined modeling framework is developed, including an element-wise solution–diffusion model for RO and system-level models for AGMD, PTC, and the spray dryer. The model predicts freshwater production, energy consumption, and salt recovery under varying operating conditions. At a feed flow rate of 16,000 L/h, the hybrid system produces approximately 9,300 L/h of freshwater, compared to 4,800 L/h for a standalone RO system. Although electrical energy consumption increases from 19 to 23.5 kWh/day, solar thermal input improves overall efficiency. The system achieves up to 135 kg/h of solid salt with product water quality below 500 mg/L TDS. The proposed system offers improved water recovery, effective brine management, and a sustainable solution for water-scarce regions.

Cite this article: Moradalizadeh, P., Zarei, T., Abedini, E., Khorshidi, J., (2026), Design and Thermodynamic Evaluation of An Integrated RO-AGMD-Spray Dryer System for Solar-Powered Zero Liquid Discharged Desalination, *Chemical Process Design*, 6(1), 1-14. http//doi.org/10.22111/cpd.2026.56159.1098

© The Author(s).
DOI: http//doi.org/10.22111/cpd.2026.56159.1098

Publisher: University of Sistan and Baluchestan.

ARTICLE IN PRESS

1. Introduction

1.1 Research Background and Motivation

Freshwater is a vital resource for human consumption, industrial operation and economic development. The World Health Organization (WHO) recommends drinking water contain a concentration of dissolved substances (TDS) below 500 mg/L to be safe. Around 96.5–97% of water is saline in the oceans with TDS greater than 35,000 ppm and not available readily for direct use, while only about 2–3% water exists as freshwater in lakes, glaciers, ice caps etc. This scarcity, together with rapid population growth, economic growth and climate change are rendering these regions water stressed with forecasts that, by 2030, the global demand for freshwater will outstrip supply by as much as 40% [1].

Desalination has become a viable process for the drinking water supply as it is difficult to satisfy the insatiable demand for drinking water in water-stressed regions and there are limited resources of freshwater. Desalination technologies separate dissolved salts and contaminants from saline water, however traditional processes such as reverse osmosis (RO), multi-stage flash (MSF) and multi-effect distillation (MED) are power demanding and fossil fuel based resulting in high cost of operation and environmental pollution [2]. Lately, several studies have focused on combining renewable energy sources for the purpose of offshore desalination plants power supply. Literature indicates that solar-assisted desalination, especially when integrated with membrane processes, will reduce power consumption substantially and improve the overall process efficiency [3].

A significant problem with desalination is the handling of brine that is produced, and discharge to sea can result in environmental implications. In order to solve the brine disposal problem, zero liquid discharge (ZLD) technologies have appeared in recent years as sustainable process to eliminate all liquid effluent along with recovery of valuable salts. These processes generally include integrated desalting combined with advanced concentration and evaporation techniques for highest water and salt recovery. For instance, combination of photovoltaic (PV) or solar thermal with evaporation systems can enable the production of freshwater and solid salts from brine to operate ZLD mode [4].

The use of solar energy in desalination, particularly in areas that receive abundant sunlight such as Iran and other arid regions, decreases not only the consumption of fossil fuels but also greenhouse gas emissions and costs. Various works have shown that solar-thermal and solar-PV hybrid desalination systems can provide a feasible, sustainable, and economic alternative for the production of potable water at different scales[3, 5, 6]. Accordingly, the further development of desalination technologies using renewable energy can potentially make a significant contribution to water security in arid and semi-arid areas as well as sustainable development goals.

While numerous publications have reported extensively on forms of individual desalination processes such as reverse osmosis (RO) and membrane distillation (MD), including their partial hybridization with renewable energy sources, most studies are centered on standalone configurations or short-branched hybrid centralization [1-3]. Several studies have developed solar driven desalination, and zero liquid discharge concepts, but most of them dealt with only freshwater production and brine minimization separately rather than to provide an integrated system that enhances water recovery while reducing the specific energy demand that guarantee a complete elimination of liquid brine [4, 5, 7].

As per the authors' search, there is no detailed thermodynamic study of such a coupled RO–AGMD–spray dry desalination system fueled by solar thermal energy with ZLD practice in existence in the open literature. To this end, the objective of this study is to bridge such a gap by proposing a unique thermodynamic approach to evaluate the overall system performance, freshwater recovery rate and energy efficiency, and salt recovery potential.

ARTICLE IN PRESS

1.2 Literature Review

1.2.1 Overview of Desalination Technologies

Sharqawy et al. [8] performed a general survey of early thermal desalination technologies, focusing on multi-stage flash (MSF) and multi-effect distillation (MED). These systems were primarily used in regions with abundant energy resources, but they consumed high energy (typically 80–120 kWh/m³) and faced sustainability issues. Crucially, Tarif et al. [1] discussed that desalination technology significantly advanced with the implementation of reverse osmosis (RO) in the 1970s. RO membranes offered considerably higher energy efficiency (around 3–6 kWh/m³) and greater flexibility in system sizing compared to thermal processes.

AL-Ghamdi et al. [9] reported that modern RO plants can achieve freshwater recovery up to 50%. However, they emphasized that brine production remains a major challenge, highlighting the need for efficient brine management strategies. Moreover, Chen et al. [10] demonstrated in pilot-scale studies that integrating energy recovery devices can further increase RO plant energy efficiency by up to 40% while maintaining high product water quality.

1.2.2 Renewable Energy Integration in Desalination

AL-Ghamdi et al. [9, 11] emphasized the integration of solar energy, including both photovoltaic (PV) and solar thermal technologies, with reverse osmosis (RO) or other desalination processes to reduce reliance on fossil fuels and lower CO_2 emissions. Their results indicated that 60–70% of the energy demand in decentralized desalination systems could be met by solar-driven RO.

Chen and Ng [12] developed a solar thermal energy-driven zero liquid discharge (ZLD) system to enhance the energy efficiency of multi-effect distillation (MED) coupled with evaporative crystallization. Menon et al. [6] investigated solar energy-driven distributed desalination systems, showing that hybrid configurations, such as PV-wind or PV-thermal, can effectively overcome intermittency issues and ensure a continuous 24/7 supply of freshwater.

Zarei and Miroliaei [13] analyzed a small-scale HDH desalination system with direct contact towers, demonstrating that optimized operating conditions can achieve a GOR of up to 3.3 and produce about 300 L/day of freshwater, making it suitable for domestic applications.

Chen et al. [10] demonstrated that specific energy consumption (SEC) can be reduced by 30–50% in solar-augmented desalination systems compared to conventional RO, thereby promoting sustainable water supply in arid regions.

1.2.3 Hybrid Desalination Systems

Accurate thermal modeling of parabolic trough solar collectors is essential for predicting the performance of solar-driven desalination systems. Particularly, Nayal et al. [14] highlighted the importance of hybrid configurations integrating thermal energy with membrane processes. Chen et al. [10] developed a novel hybrid RO-MD system coupled with solar thermal energy, achieving a freshwater recovery of 60–65% per unit of feedwater treated. Similarly, Gadalla et al. [5] established a hybrid zero-liquid discharge (ZLD) system using RO followed by air-gap membrane distillation (AGMD). Their study demonstrated that this configuration can remove up to 70% of brine while producing solid salts as a valuable by-product.

Chen et al. [10] reported that integrating AGMD with RO enables the treatment of brine streams at high salinity, with total dissolved solids (TDS) levels up to 120,000 ppm, which is otherwise challenging for conventional RO systems.

ARTICLE IN PRESS

Moreover, AL-Ghamdi et al. [9, 11] found that hybrid solar-membrane systems significantly enhance energy efficiency and freshwater recovery, making these technologies particularly suitable for remote or semi-arid regions. Advanced and enhanced reverse osmosis configurations have also been proposed as viable pathways toward minimal and zero liquid discharge, particularly when combined with downstream brine concentration technologies [15].

1.2.4 Brine Management and Zero Liquid Discharge (ZLD)

Thermodynamic and exergy analyses further reveal that hybrid desalination systems offer superior energetic performance compared to standalone processes, enabling more efficient utilization of renewable energy sources [16]. Al-Sulaiman et al. [17] investigated various advanced brine concentration and crystallization processes, demonstrating that salts can be recovered with high efficiencies (up to 90%) while minimizing environmental impact. Shi et al. [7] reported that spray drying can eliminate all liquid brine, producing high-purity salts suitable for commercial applications. Chen and Ng [12] developed a ZLD system based on multi-effect distillation, evaporative crystallization, and thermal vapor compression, capable of reusing nearly 100% of the water content. AL-Ghamdi et al. [9] emphasized that ZLD integration not only enhances resource utilization and ensures compliance with environmental regulations but also allows optimization of energy inputs through renewable energy sources. Recently, electrified solar zero liquid discharge (PV-ZLD) systems have gained increasing attention, demonstrating strong potential for integrating photovoltaic energy with advanced brine management strategies in large-scale desalination plants [18].

1.2.5 Membrane Distillation and Advanced Configurations

Al-Obaidani et al. [19] demonstrated the feasibility of treating high-salinity brine using AGMD with low-temperature waste heat, achieving water recovery rates above 60% for brine streams unsuitable for conventional RO. Chen and Ng [12] suggested that integrating AGMD with RO can increase total freshwater recovery by 15–20% while enabling ZLD operation. Chen et al. [10] reported that solar-driven hybrid systems combining RO and AGMD operate efficiently with minimal brine discharge, supporting sustainable water treatment in arid and semi-arid regions. Comprehensive reviews on hybrid membrane distillation systems indicate that coupling MD with RO or thermal desalination processes significantly enhances overall water recovery while reducing specific energy consumption [20].

1.2.6 Spray Drying and Salt Recovery

Chen and Ng [12] and Fernandez et al. [21] investigated spray drying in closed-circuit desalination systems, showing that salt recovery can reach 85% or higher while removing all liquid waste and producing industrial-grade salts. AL-Ghamdi et al. [9] highlighted that coupling spray drying with solar-driven hybrid desalination systems achieves full ZLD operation, maximizing both freshwater and salt recovery.

1.2.7 Energy Efficiency, SEC, and Thermodynamic Modeling

ARTICLE IN PRESS

Sharqawy et al. [8] developed thermodynamic models for desalination systems based on mass and energy balances, heat and mass transfer, and membrane transport relations. These models have been applied by Wang et al. [4] and Gadalla et al. [5] to optimize hybrid RO–AGMD systems, achieving a 20–40% reduction in specific energy consumption (SEC) compared with conventional RO. Chen et al. [10] demonstrated that predictive thermodynamic modeling is a valuable tool for designing systems with high freshwater recovery and improved energy efficiency.

1.2.8 Research Gaps and Unexplored Opportunities in Solar-Driven Hybrid Desalination

While considerable progress has been made in the field of desalination and the development of hybrid solar-driven systems, several research challenges remain. Most studies have focused on standalone desalination techniques, such as reverse osmosis (RO) and membrane distillation (MD), or on partial hybrid systems integrating solar energy [19, 22]. Although hybrid systems combining RO with air-gap membrane distillation (AGMD) have been explored, a comprehensive analysis covering all stages—including RO, AGMD, and spray drying for zero liquid discharge (ZLD)—is still lacking [21, 23].

Previous research often treats freshwater production and brine minimization as separate issues rather than developing an integrated system that maximizes water recovery, minimizes specific energy consumption, and ensures complete brine elimination [7, 12]. Harby et al. [24] review hybrid RO systems and highlight their potential to increase water recovery and reduce energy use. However, they do not present a fully integrated RO–AGMD–spray dryer system powered by solar thermal energy for complete freshwater and salt recovery.

Addressing this gap could significantly improve the sustainability and efficiency of desalination in semi-arid and arid regions. It may enable higher freshwater recovery, full salt recovery, and environmentally compliant brine management using renewable energy sources. This background underlines the motivation for the present study, which aims to develop a thermodynamic modeling framework for an integrated solar-driven hybrid desalination system operating under ZLD conditions.

To clearly articulate the novel contribution of this work, the conceptual framework behind the system configuration should be highlighted. Because reverse osmosis is the most widely adopted and proven industrial technology for seawater desalination, it is strategically implemented as the baseline treatment stage. To sustainably process the resulting concentrated brine, air gap membrane distillation is introduced as a compatible secondary stage, effectively utilizing thermal driving forces to treat high-salinity effluent that exceeds the operational limits of pressure-driven membranes. In the final stage, to fully mitigate environmental concerns associated with liquid brine disposal, a vacuum spray dryer is employed as an efficient, rapid crystallization mechanism to recover solid salts and achieve complete zero liquid discharge. Additionally, a parabolic trough solar collector field supplies the requisite thermal energy, thereby curbing operational expenditure and dependence on fossil fuels. The simultaneous multi-scale thermodynamic coupling and comprehensive energy assessment of this fully integrated RO–AGMD–spray dryer chain powered by solar thermal energy represent the core novelty of this investigation, which has not been previously addressed.

2. Methodology and System Modeling

ARTICLE IN PRESS

2.1 Overview of the Hybrid System and Modeling Approach

The hybrid desalination system in this study integrates a reverse osmosis (RO) unit, an air-gap membrane distillation (AGMD) module, and a vacuum spray dryer powered by a parabolic trough collector (PTC). To capture both detailed RO performance and system-level behavior, a multi-scale modeling approach is adopted:

1. Element-wise physical model for RO: Accurate calculation of water flux, salt transport, and recovery for each membrane element.
2. System-level model for AGMD, PTC, and spray dryer: Linear scaling from reference conditions to predict freshwater output, solar energy demand, and solid salt recovery.

The framework predicts key outputs including freshwater production, solid salt recovery under zero liquid discharge (ZLD), and total electrical and solar energy consumption. Simulations are performed under steady-state conditions, and feed water is modeled as an equivalent NaCl solution representing seawater [8, 25].

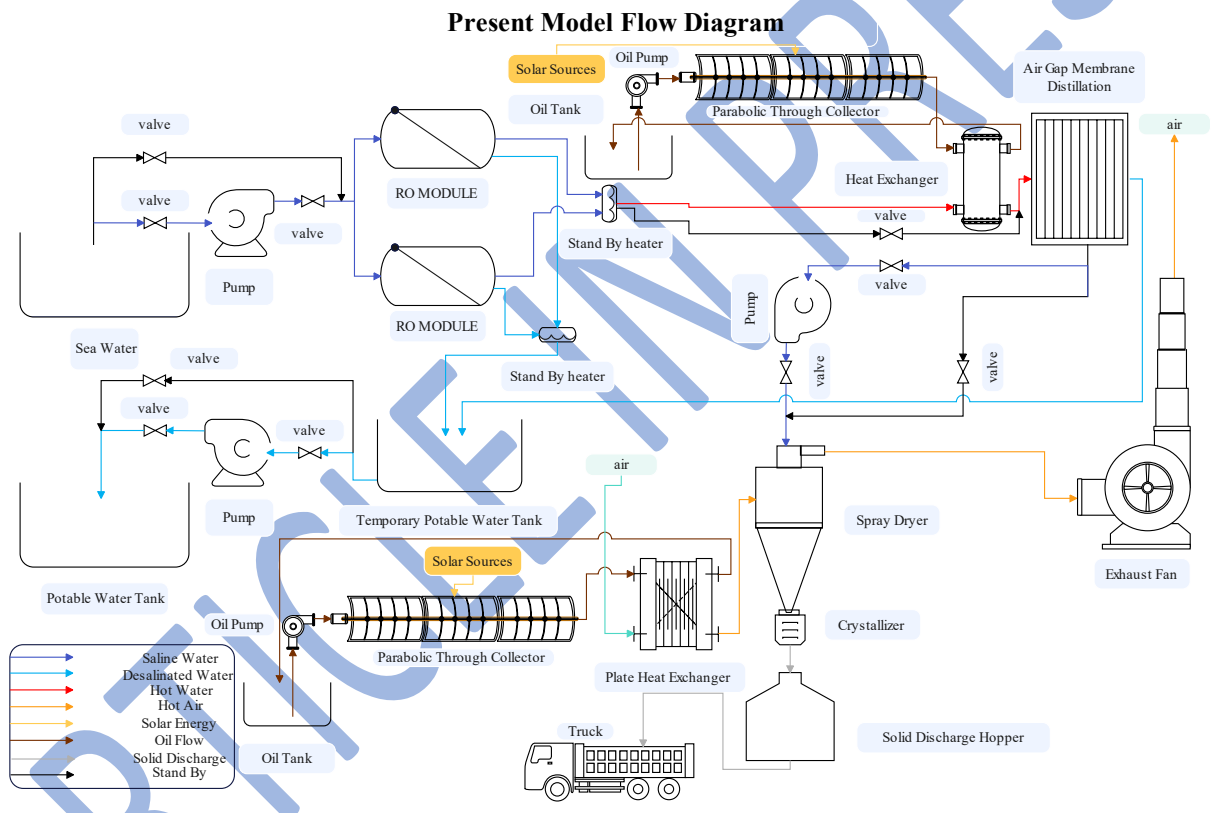


Fig. 1. Schematic diagram of the hybrid RO–AGMD–Spray Dryer desalination system.

As it is shown in Fig. 1, the system investigated in this study is a hybrid desalination and salt recovery process designed for simultaneous freshwater production and zero liquid discharge (ZLD). The proposed configuration integrates reverse osmosis (RO), air gap membrane distillation (AGMD), and a spray dryer in a single process chain. Seawater with a total dissolved solids (TDS) concentration of approximately 35 g/L is supplied to the RO unit as the primary desalination step, where the majority of freshwater is recovered. The concentrated brine exiting the RO unit is subsequently directed to the AGMD module to further enhance water recovery and reduce the volume of the final brine stream.

ARTICLE IN PRESS

The thermal energy required for AGMD operation is supplied by a solar parabolic trough collector (PTC), while electrical energy is mainly consumed by high-pressure pumps and auxiliary equipment. The highly concentrated brine leaving the AGMD unit is finally treated in a spray dryer, where complete evaporation of the remaining water enables recovery of dissolved salts in solid form. This hybrid RO–AGMD–spray dryer configuration allows high overall water recovery, reduced environmental discharge, and partial substitution of fossil-based energy with solar thermal input. The system is numerically modeled using a detailed membrane-element-based RO model coupled with a system-level representation of the AGMD, solar collector, and spray dryer units, enabling performance evaluation under various feed flow rate scenarios.

2.2 Reverse Osmosis Unit Modeling

2.2.1 Assumptions

The RO unit is discretized into N_{membrane} elements along the axial direction. The following assumptions are applied:

- One-dimensional, steady-state flow.
- Constant water permeability (A_w) and salt permeability (B) coefficients [8, 25].
- Linear pressure drop along the vessel.
- Negligible temperature variation.
- Equivalent NaCl representation of feed salinity.
- Concentration polarization modeled empirically as a function of element recovery.

2.2.2 Water Flux

Water flux for element i is calculated using the solution-diffusion model:

$$J_{w,i} = A_w \cdot FF \cdot \Delta P_{\text{eff},i} \tag{1}$$

where:

- A_w = water permeability coefficient (L/(m²·h·bar))
- FF = fouling factor
- $\Delta P_{\text{eff},i}$ = effective transmembrane pressure

Effective transmembrane pressure is defined as:

$$\Delta P_{\text{eff},i} = \left(P_{f,i} - P_p - \Delta P_{\text{half},i}\right) - \left(\pi_{c,\text{avg},i} - \pi_p\right) \tag{2}$$

where:

- $P_{f,i}$ = feed pressure at element i
- P_p = permeate pressure
- $\Delta P_{\text{half},i}$ = pressure drop across the element
- $\pi_{c,\text{avg},i}$, π_p = osmotic pressures of concentrate and permeate, respectively [8, 25].

2.2.3 Osmotic Pressure and Concentration Polarization

Osmotic pressure is calculated via van 't Hoff equation:

ARTICLE IN PRESS

$$\pi = i_{vh} \cdot C_{mol} \cdot R_g \cdot T \tag{3}$$

The concentration at the membrane-feed interface, accounting for polarization:

$$C_{fc,i} = C_{f,i} \cdot \frac{ln\left(1/\left(1-R_i\right)\right)}{R_i}, CP_i = exp\left(0.7 \cdot R_i\right), C_{m,i} = C_{fc,i} \cdot CP_i \tag{4}$$

where R_i is the element recovery ratio.

2.2.4 Salt Transport

Permeate salt concentration is:

$$C_{p,i} = \frac{C_{m,i}}{1 + \frac{J_{w,i}}{B_{eff}}} \tag{5}$$

Element-wise mass balances:

$$Q_{p,i} = J_{w,i} \cdot A_{m,i} \tag{6}$$

$$Q_{c,i} = Q_{f,i} - Q_{p,i} \tag{7}$$

$$C_{f,i+1} = \frac{C_{f,i}Q_{f,i} - C_{p,i}Q_{p,i}}{Q_{c,i}} \tag{8}$$

The overall recovery ratio:

$$R_{total} = \frac{\sum_{i=1}^{N} Q_{p,i}}{Q_{f,1}}. \tag{9}$$

Feed pressure is iteratively adjusted using a bisection method to achieve the target recovery [8, 25].

2.3 System-Level Modeling of AGMD and PTC

The AGMD and solar PTC are represented at system level, calibrated using reference operating conditions. Freshwater production and solar energy demand are scaled linearly with feed flow Q_0 [2, 9]:

$$Q_{fw,AGMD}\left(Q_0\right) = Q_{fw,AGMD,ref} \cdot \frac{Q_0}{Q_{0,ref}} \tag{10}$$

$$E_{solar}\left(Q_0\right) = E_{solar,ref} \cdot \frac{Q_0}{Q_{0,ref}} \tag{11}$$

The PTC provides steady thermal input to the AGMD module, with no dynamic heat loss considered [2, 5].

2.4 Spray Dryer Modeling and ZLD

The spray dryer ensures full recovery of salts, consistent with zero liquid discharge (ZLD) operation [4, 22, 26]. Salt mass balance:

$$\dot{m}_{salt,in} = C_{salt} \cdot Q_0 \tag{12}$$

$$\dot{m}_{salt,solid} = \dot{m}_{salt,in} \tag{13}$$

ARTICLE IN PRESS

Residual liquid is assumed negligible. This approach aligns with the design of solar-driven vacuum spray dryers for ZLD desalination.

3. Data and model validation

3.1 Data Scope and Sources

The hybrid RO–AGMD–Spray Dryer desalination system is calibrated and validated against reference data reported in the literature. The primary aim of this section is to describe the data sources, reference operating conditions, and calibration procedure used for the system-level and RO element-wise models .The reference operating point corresponds to a feed flow rate of Q0,ref = 2000 L/h with the following reported values [26]:

- RO permeate flow: $Q_{fw,RO,ref} \approx$ 1500 L/h
- AGMD permeate flow: $Q_{fw,AGMD,ref} \approx$ 425 L/h
- Total electrical energy consumption: $E_{el,ref} \approx$ 1000 kWh/day
- Solar thermal input from parabolic trough collector: $E_{solar,ref} \approx$ 350 kWh/day
- Feedwater salinity: $C_{salt,in}$ = 35000 mg/L = 0.035 kg/L

These reference data form the basis for calibrating both the detailed RO model and the system-level AGMD and Spray Dryer modules. Additional reference data for validation and comparison are taken from published literature, including SW30HR membranes reported by Altaee [۲۷] for RO performance and Hamawand et al. [26] for vacuum spray dryer behavior.

3.2 RO model validation

The RO element-wise model is calibrated using the feedwater salinity and target recovery ratios defined in the reference scenario. The calibration ensures that element-level water flux, salt transport, and overall recovery match the reference operating point. The calibration procedure involves iteratively adjusting the feed pressure using the bisection method until the overall recovery satisfies $R_{total} \approx 0.30$ (Eq. (9))

Elemental water flux, concentration polarization, and permeate salt concentration are calculated as described in Eqs. (1)–(5), with element-wise mass balances according to Eqs. (6)–(8). The calibration ensures consistency between modeled and reference permeate flows and feed/retentate concentrations.

Membrane parameters for SW30HRLE-400i and SW30HR-380 are assigned according to literature values and adjusted slightly to reproduce the reference scenario.

3.3 System-Level AGMD and PTC validation

The AGMD module and parabolic trough collector are represented using a system-level scaling approach. Reference operating values are used to define linear scaling coefficients for permeate production and solar energy consumption with respect to feed flow Q_0 (Eqs. (10) and (11)):

$$Q_{fw,AGMD}(Q_0) = Q_{fw,AGMD,ref} \cdot \frac{Q_0}{Q_{0,ref}} \tag{14}$$

$$E_{solar}(Q_0) = E_{solar,ref} \cdot \frac{Q_0}{Q_{0,ref}} \tag{15}$$

ARTICLE IN PRESS

These relations allow estimation of AGMD permeate and solar input for different feed flow rates without solving detailed heat and mass transfer equations. The scaling approach has been validated against reference data and is appropriate for the range of flows considered.

To evaluate transport phenomena within the AGMD module beyond linear scaling, localized heat and mass transfer mechanisms are modeled according to Eqs. (16) and (17) following the formulation by Winter [28]. The total mass flux across the membrane and the air gap ($j_{\text{L-AG}}$) is governed by combined diffusion and viscous flow regimes:

$$j_{L-AG} = j_{L-AG,d} + j_{L-AG,v} = C_{L-AG,d}\left(p_{W,1} - p_{W,0}\right) + C_{L-AG,v}\left(\hat{p}_1 - \hat{p}_0\right) \tag{16}$$

where $C_{\text{L-AG,d}}$ and $C_{\text{L-AG,v}}$ denote the mass transfer coefficients for diffusion and viscous flow, respectively, while $p_{\text{w,1}}$ and $p_{\text{w,0}}$ are the partial vapor pressures at the respective boundary interfaces. Concurrently, the total heat transfer rate across the composite layers ($\dot{q}_{\text{L-AG}}$) is calculated using Eq. (1٧):

$$\dot{q}_{L-AG} = j_{L-AG}\Delta h_v + \left[\frac{\delta_M}{\lambda_M^*} + \frac{\delta_B}{\lambda_B^*} + \frac{\delta_{AG}}{\lambda_{AG}^*}\right]^{-1}\left(T_1 - T_0\right) + \frac{\varepsilon_{AG}\delta}{\epsilon_M^{-1} + \epsilon_W^{-1} - 1}\left(T_1^4 + T_0^4\right) = k_{L-AG}\left(T_1 - T_0\right) \tag{17}$$

where Δh_{v} is the latent heat of vaporization, δ and λ^* represent the effective thickness and thermal conductivities of the membrane, boundary layer, and air gap, ε is the surface emissivity, and σ is the Stefan–Boltzmann constant.

3.4 Spray Dryer and ZLD Salt Balance

The spray dryer is modeled to achieve full recovery of salts in a zero liquid discharge (ZLD) configuration. Salt mass balance follows Eqs. (12) and (13) that all dissolved salts in the feedwater are recovered as solid salt. This procedure allows calculation of solid salt production as a function of feed flow rate and facilitates comparison with reference literature.

3.5 Data Implementation for Sensitivity Analysis

For system-level analysis and sensitivity studies:

1. Define a set(vector in MATLAB) of feed flow rates Q_0 ranging from 500 to 4000 L/h.
2. Compute the scaling factor $\text{scale} = Q_0 / Q_{0,\text{ref}}$.
3. Calculate scaled RO and AGMD permeate using the reference values [26] and Eqs. (10) and (11).
4. Compute total permeate flow $Q_{\text{fw,total}} = Q_{\text{fw,RO}} + Q_{\text{fw,AGMD}}$.
5. Calculate solid salt production using Eqs. (12) and (13).
6. Scale electrical and solar energy consumption linearly with feed flow Eqs. (14) and (15).

The resulting dataset forms the basis for generating tables and plots for total permeate, solid salt production, and energy consumption over a range of operating conditions.

3.6. Computational Implementation and Data Referencing

3.6.1 Programming Environment

All numerical simulations presented in this study were implemented using MATLAB. The computational framework consists of modular scripts and user-defined functions for RO simulation, pressure calibration, system-level scaling,

ARTICLE IN PRESS

and post-processing. MATLAB was selected due to its numerical robustness, matrix-handling capability, and suitability for iterative solution of nonlinear algebraic equations. In addition to MATLAB, data processing and post-analysis in this study were performed using the Python programming language, with NumPy for numerical computations [29], Pandas for structured data handling [30], and Matplotlib for data visualization and plotting [31].

3.6.2 Data Referencing and Literature Sources

Model parameters and reference performance data for the RO unit were obtained from this study and relevant membrane literature. System-level data related to spray drying and salt recovery were referenced from published studies on solar-driven spray dryer desalination systems [26].

4. Results and discussion

This section presents the simulation results and analysis of the three-stage solar-driven hybrid RO–AGMD–ZLD system. The proposed coupled system is first compared with conventional RO in terms of freshwater production (Fig. 2) and electrical energy consumption (**Fig. 3** and **Fig. 5**).

The thermal performance of the solar sub-system is then evaluated, including PTC efficiency (Fig. 6), required aperture area (Fig. 7), and thermal energy supply (Fig. 8). The AGMD unit is validated through water flux comparisons (Fig. 10) and product water quality against experimental data (Fig. 14).

Finally, the ZLD component is assessed via salt outlet rate (Fig. 12) and total solid salt production (Fig. 13), confirming the overall reliability, efficiency, and sustainability of the hybrid system.

4.1 Overall System Comparison (Water Output vs. Electrical Input)

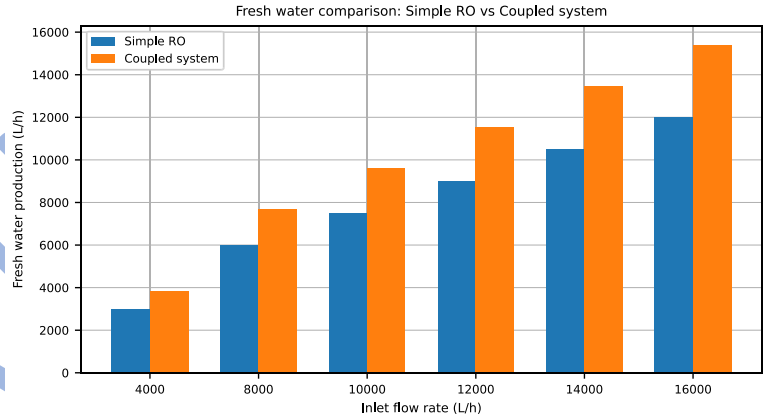


Fig. 2. Comparison of freshwater production vs. feed water flow rate (conventional RO utilizing Altaee [۲۷] membrane specifications vs. the proposed coupled system)

Fig. 2 presents the comparative performance of freshwater production (L/h) between the conventional RO system utilizing SW30HR membranes reported by Altaee [۲۷] (blue bars) and the proposed coupled system (orange bars) across the full range of feed water flow rates (Q_{in}, from 4000L/h up to 16000 L/h). The visual confirmation provided by this bar chart emphatically validates the superior productivity of the hybrid design [2, 10]. At every discrete operating point, the proposed coupled system consistently achieves a substantially higher freshwater output than its conventional RO counterpart. For instance, the difference is particularly pronounced at the maximum tested capacity

ARTICLE IN PRESS

(16000 L/h) where the proposed coupled system's production significantly exceeds that of the conventional RO. This outcome confirms the efficacy of integrating the solar-driven AGMD unit to treat the RO reject brine, enabling the system to reach a maximum overall Water Recovery Rate (WRR) far beyond the limitations imposed by the scaling threshold of the conventional RO stage alone. Therefore, this figure confirms that the proposed coupled system successfully fulfills its primary objective: maximizing clean water production across various scales of operation.

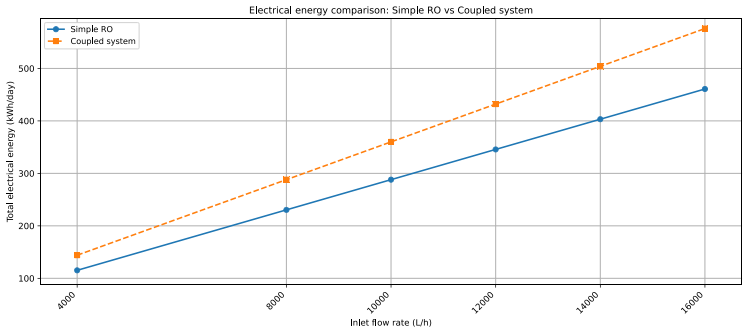


Fig. 3. Comparison of total electrical energy consumption vs. feed water flow rate (conventional RO utilizing Altaee [۲۷] membrane specifications vs. the proposed coupled system)

Fig. 3 details the comparison of Total Electrical Energy Consumption (kWh/day) versus the Feed Water Flow Rate (L/h) for the conventional RO utilizing Altaee [۲۷] membrane specifications and the proposed coupled system. Similar to the output comparison in Fig. 3, both systems exhibit a proportional, linear increase in total energy consumption as the water flow rate is raised. However, in contrast to the water output, the proposed coupled system consistently demands a higher total electrical energy input than the conventional RO system across the operating range. For example, at a maximum feed rate of 16,000 L/h, the proposed coupled system's total electrical consumption reaches approximately 23.5 kWh/day, compared to about 19 kWh/day for the conventional RO system. This expected increase in total power demand is due to the auxiliary equipment (pumps, etc.) needed to drive the higher overall throughput and the additional process units in the coupled configuration. Crucially, the system is designed to use solar thermal energy (from the PTC) to power the subsequent AGMD stage, which offsets the need for electrical energy in that high-salinity processing step [3, 6]. Therefore, while the total electrical load is higher, the primary measure of efficiency for this hybrid design is the Specific Electrical Energy Consumption (SEC) per unit of produced freshwater, which is expected to be competitive or lower due to the significant contribution of renewable solar thermal energy [1, 26].

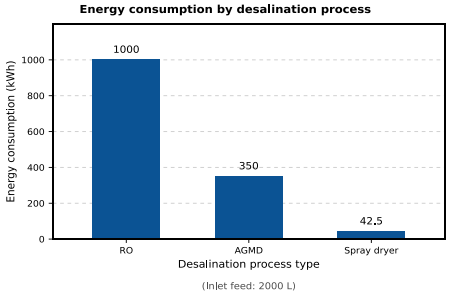


Fig. 4. Specific energy consumption (SEC) breakdown across the individual subsystems (RO, AGMD, and spray dryer) under reference operating conditions ($Q_{in} = 2,000$ L/h).

ARTICLE IN PRESS

As depicted in Fig. 4 , the system's energy requirement is presented by process stage at a specific volumetric flow rate, reflecting the individual energy consumption of each operational unit. The reverse osmosis (RO) process alone accounts for more than 70% of the total system energy demand. Therefore, to curtail energy consumption within the designed configuration, a larger portion of the desalination load can be shifted to the AGMD process. This operational flexibility contributes to a substantial reduction in overall desalination energy requirements. Furthermore, employing membranes with higher permeability can be considered, which diminishes operating resistance, extends membrane service life, and ensures sustained separation performance over longer operating periods.

To account for membrane fouling effects and evaluate the internal energy distribution, an element-wise discretization scheme was implemented in the simulation framework. Dividing the RO module into $N_{membrane}$ axial control volumes enables the model to solve localized mass and energy balances for each element. This allows progressive variations in salinity, effective permeability, localized fouling resistance, and osmotic back-pressure to be updated along the vessel length. Consequently, this discretization strategy ensures robust numerical convergence and yields excellent agreement between the predicted RO performance and experimental reference data.

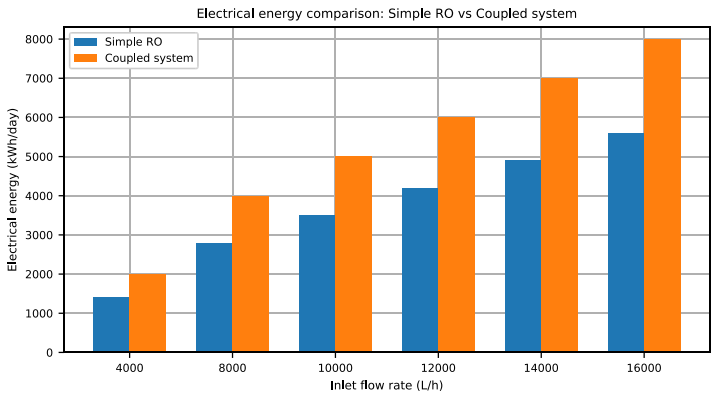


Fig. 5. Total electrical energy consumption (kWh/day) vs. feed water flow rate (bar chart) – conventional RO utilizing Altaee [۲۷] membrane specifications vs. the proposed coupled system

Fig. 5 presents the comparison of the total daily electrical energy consumption (kWh/day) between the conventional RO system utilizing Altaee [۲۷] membrane specifications (blue bars) and the proposed coupled system (orange bars) across various feed water flow rates (4000 L/h to 16000L/h). Consistent with the trends observed in the line plot (Fig. 4), this bar chart confirms that the proposed coupled system consistently demands a higher absolute electrical energy input than the conventional RO system at every flow rate. For example, at 16000 L/h, the proposed coupled system consumes over 7500 kWh/day, significantly more than the conventional RO system's 5600 kWh/day. This increase in electrical demand is a direct consequence of the additional pumps and components required to power the secondary AGMD stage and achieve high water recovery. Therefore, while the proposed coupled system more water (Fig. 9), its economic justification rests on the contribution of the integrated solar thermal energy, which significantly reduces the Specific Electrical Energy Consumption (SEC) per unit of freshwater produced.

4.2 Solar Thermal Sub-System Analysis (PTC)

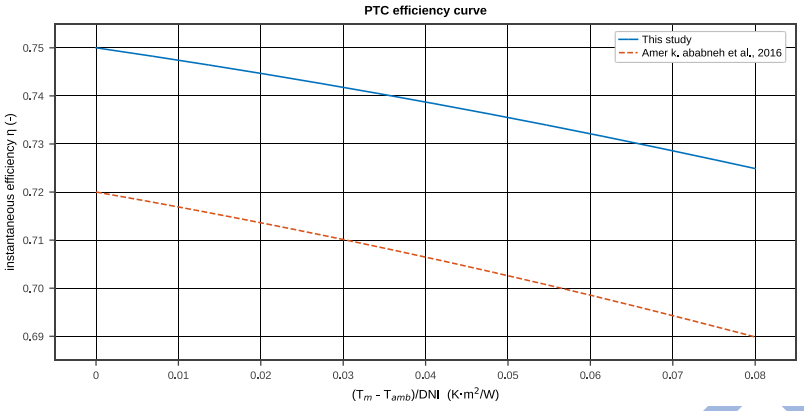


Fig. 6. Instantaneous thermal efficiency of PTC vs. reduced temperature $(T_m - T_{amβ}) / DNI$ – this study vs. Ababneh et al. [32]

Fig. 6 illustrates the comparative instantaneous thermal efficiency (η) of the Parabolic Trough Collector (PTC) employed in this study and a reference PTC reported by Ababneh et al. [32], plotted as a function of the standard efficiency parameter $(T_m - T_{amβ}) / DNI$, where T_m denotes the mean fluid temperature, $T_{amβ}$ is the ambient temperature, and DNI represents the direct normal irradiance. This parameter is commonly used to evaluate thermal losses under different operating temperature conditions.

The results indicate that the modeled PTC exhibits a consistently higher instantaneous thermal efficiency over the entire operating range when compared to the reference PTC [32]. In particular, the optical efficiency, represented by the y-intercept at $(T_m - T_{amβ}) / DNI = 0$, is approximately 0.75 for the modeled PTC, whereas the reference PTC [32] shows a lower value of about 0.72.

The improved thermal performance of the proposed PTC is of significant importance, as it directly enhances the thermal energy supplied to the AGMD unit. Higher solar collection efficiency ensures a more stable and sufficient heat input, leading to increased AGMD freshwater production and improved overall thermal and exergy efficiencies of the integrated hybrid desalination system.

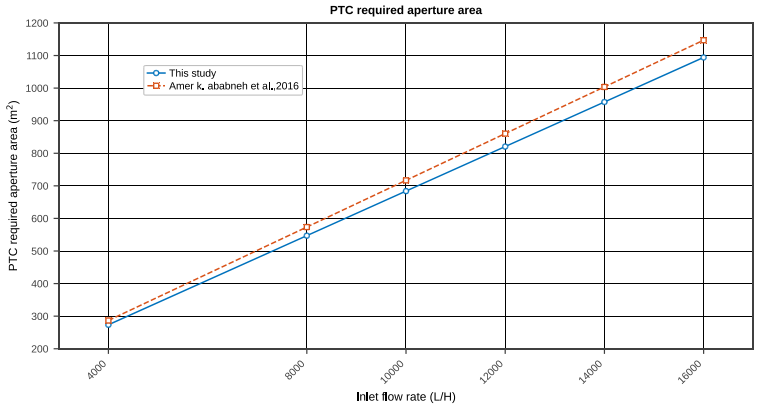


Fig. 7. Required PTC aperture area (m²) vs. feed water flow rate (L/h) – this study vs. Ababneh et al. [32]

Fig. 7 compares the necessary Parabolic Trough Collector (PTC) aperture area (in m٢) to meet the thermal load for the coupled system's AGMD unit, between the PTC modeled in this study and the PTC referenced from an external

ARTICLE IN PRESS

study [32]. The X-axis plots the Feed Water Flow Rate (L/h), and the Y-axis shows the Required PTC Aperture Area (m^2). Both lines demonstrate a strong linear dependency, showing that the required collector area increases directly with the overall feed rate, as a larger flow rate demands a greater thermal load to drive the desalination process.

The key finding from this comparison is that the PTC modeled in this study (blue line) requires a consistently smaller aperture area than the PTC reported by Ababneh et al. [32] (orange line) to supply the identical thermal load at every feed flow rate. For instance, at a feed rate of 16,000 L/h, the required area for the PTC in this study is approximately 1,090 m^2, whereas the system by Ababneh et al. [32] requires around 1,140 m^2 This difference directly correlates with the superior thermal efficiency demonstrated by the PTC in this study (Fig. 6). A smaller required aperture area translates into lower capital costs and a smaller system footprint, significantly improving the economic viability and practical applicability of the solar-driven hybrid desalination system.

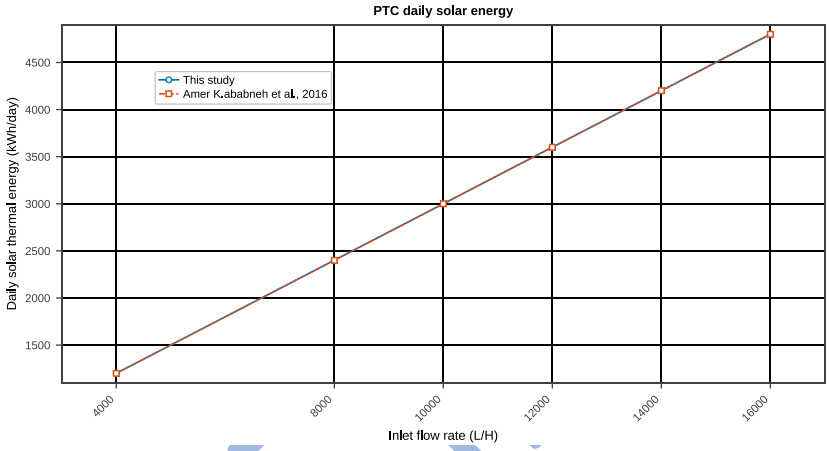


Fig. 8. Daily solar thermal energy (kWh/day) vs. feed water flow rate (L/h) for PTC – this study vs. Ababneh et al. [32]

Fig. 8 illustrates the comparison of the required daily solar thermal energy (in kWh/day) for the feed stream based on the water flow rate (L/h), comparing this study model against Ababneh et al. [32]. The X-axis represents the Feed Water Flow Rate (L/h), and the Y-axis shows the Required Daily Solar Thermal Energy (kWh/day).

The graph reveals an almost perfect alignment between the thermal energy demands calculated using the parameters of this study and those required according to Ababneh et al. [32]. Both lines demonstrate a strong, linear increase in the total required thermal energy as the feed water flow rate rises, indicating that the thermal load calculations are fundamentally consistent between the two models. For example, at the maximum feed rate of 16,000 L/h, both the model developed in this study and that of Ababneh et al. [32] require approximately 4,750 kWh/day of solar thermal energy. This near-identical required thermal energy, despite this study's PTC having a higher efficiency (Fig. 6) and smaller required area (Fig. 7), suggests that the underlying thermal load and energy balance equations used for the AGMD unit's operation are robust and well-validated against existing literature [8, 32]. This consistency confirms the accuracy of the thermodynamic model for calculating the system's thermal demand for the desalination process [8, 22].

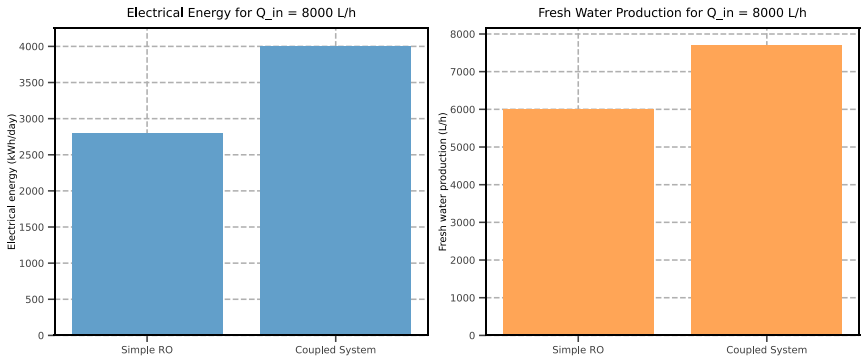


Fig. 9. Electrical energy consumption (left plot, kWh/day) and freshwater production (right plot, L/h) at a feed flow rate of 8,000 L/h for the conventional RO and the proposed coupled system

Fig. 9 compares the conventional RO and the proposed coupled systems at a fixed flow rate of 8000L/h. The charts show a fundamental trade-off: the proposed coupled system significantly increases freshwater production by nearly 30% while simultaneously requiring more total electrical energy. This demonstrates the core design objective of the hybrid architecture, maximizing water recovery, even though the increased complexity leads to a higher absolute electrical load, which is expected to be offset by the integrated solar thermal input. In this figure, a comparison of electrical energy and produced freshwater for a single flow rate is presented to simultaneously evaluate both energy consumption and produced desalinated water.

4.3 Integrated Unit Performance Validation (AGMD)

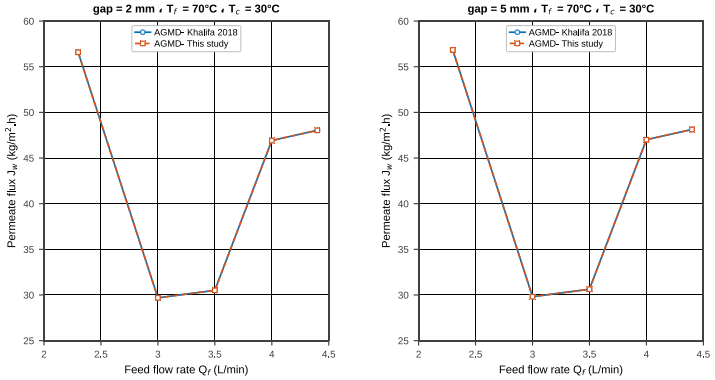


Fig. 10. Water flux (Jw, kg/m²·h) of the AGMD module versus feed flow rate (Q_f , L/min) for different air gap thicknesses (e.g., 2 mm and 5 mm) – this study vs. Khalifa [33].

Fig. 10 presents two plots validating the water flux of the Air Gap Membrane Distillation (AGMD) module as a function of feed flow rate, Q $_f$(L/min), for air gap thicknesses of 2 mm (left plot) and 5 mm (right plot). The water flux, J_w (kg/m²·h), predicted by this model (orange dashed line) is compared with a well-established AGMD model reported by Khalifa et al. [33] (blue solid line). In both cases, excellent agreement is observed across the full range of operating conditions.

The flux profiles exhibit a characteristic trend, with an initial decrease at low flow rates followed by stabilization and a subsequent increase at higher flow rates. This behavior reflects the combined effects of temperature polarization at

ARTICLE IN PRESS

low flow conditions and improved mixing with reduced concentration polarization at higher flow rates. The close overlap of the two models confirms the accuracy and reliability of the AGMD modeling approach adopted in this study, which is validated against the literature [33], supporting its use for predicting heat and mass transfer performance within the integrated hybrid desalination system.

4.4 Zero Liquid Discharge (ZLD) Performance

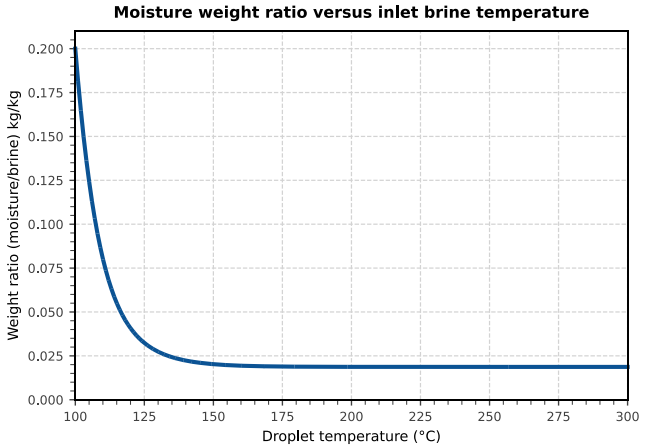


Fig. 11. Variation of droplet moisture content (W , kg/kg) as a function of droplet temperature (T_p , $^\circ$C) during the spray drying crystallization process.

The impact of thermal input and droplet temperature on drying kinetics was further evaluated within the spray drying module, as shown in Fig. 11 Droplet evaporation is strongly coupled with thermal transfer; as the droplet temperature (T_p) rises from 100°C toward the core drying threshold (140-180°C), the residual moisture content (W , in kg/kg) exhibits a sharp exponential decrease from 0.20 to less than 0.02. Beyond 180°C , the moisture removal rate stabilizes asymptotically as the final solid crystallization regime is achieved, confirming that maintaining an elevated drying chamber temperature is essential for complete moisture elimination under ZLD conditions.

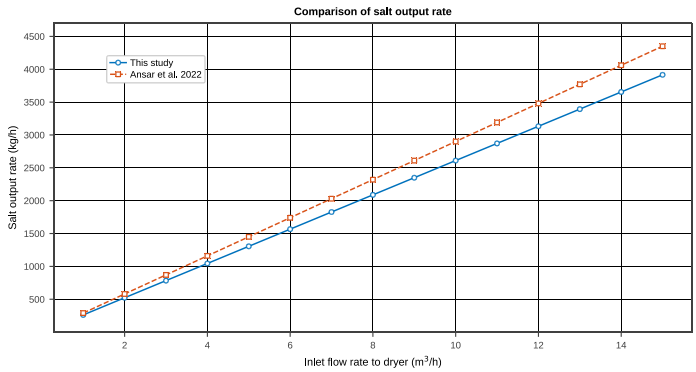


Fig. 12. Salt recovery rate (kg/h) versus feed water flow rate (m³/h), comparing the hybrid system with the reference reported by Ansar et al. [34]

ARTICLE IN PRESS

Fig. 12 compares the salt recovery performance of the hybrid system developed in this study (referred to as the Current Hybrid System) with a brine concentration system reported by Ansar et al. [34]. The figure presents the final salt outlet rate (kg/h) as a function of the feed water flow rate, Q_{in} (m^3/h). Both systems exhibit a strong linear relationship between the feed flow rate and the recovered solid salt, indicating the scalability and robustness of the Zero Liquid Discharge (ZLD) process.

A noticeable difference is observed in the magnitude of salt recovery. The system developed by Ansar et al. [34] (dashed line, C_{eff} = 0.290 kg/L) consistently produces a higher salt outlet rate than this study solid line, C_{eff} = 0.261 kg/L) at identical feed flow rates. This difference is primarily attributed to the higher effective final salt concentration achieved in the crystallization stage of the reported system [34]. Although the study of hybrid system demonstrates advantages in terms of freshwater recovery (Fig. 2) and potentially reduced required solar collector area (Fig. 7), the model proposed by Ansar et al. [34] emphasizes maximizing the final concentration limit, thereby generating a greater quantity of solid salt per unit of concentrated brine. Nevertheless, the performance of both systems confirms the technical feasibility and economic relevance of converting high-salinity brine waste into a valuable solid salt by-product, which remains a key objective of sustainable desalination strategy.

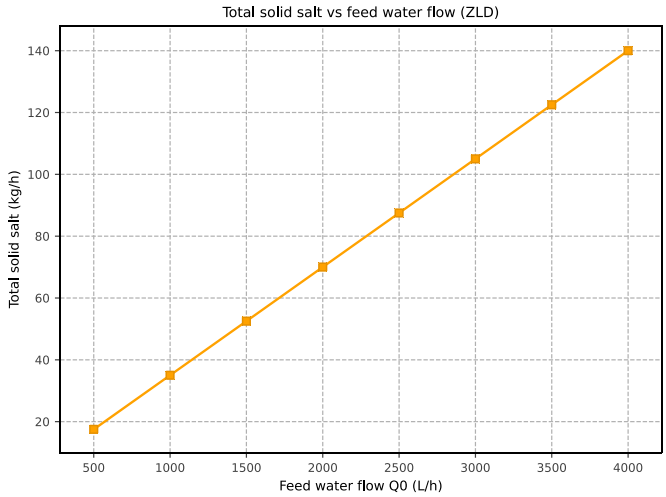


Fig. 13. Total solid salt production (kg/h) of the complete system versus feed seawater flow rate (m^3/h).

Fig. 13 illustrates the total solid salt production of the complete Zero Liquid Discharge (ZLD) process, expressed in kg/h, as a function of the incoming feed seawater flow rate, Q_{in} (m^3/h). This figure verifies the successful implementation of the ZLD concept across the full operating range of the hybrid desalination system.

The results demonstrate a strong and perfectly linear relationship between feed flow rate and total solid salt production. As the inlet seawater flow rate increases, the rate of solid salt generation rises proportionally. Specifically, salt production increases from approximately 20 kg/h at a feed flow rate of 500 L/h to nearly 135 kg/h at the maximum evaluated flow rate of 4000 L/h. This linear behavior is a direct thermodynamic consequence of constant feed salinity, where the total salt mass in the incoming stream scales linearly with volumetric flow rate. The observed trend confirms that the final crystallization stage, represented by the spray dryer, is appropriately sized and accurately modeled to process 100 percent of the rejected salt mass. As a result, the system achieves the primary environmental and economic objectives of the ZLD configuration by completely eliminating liquid brine discharge while enabling

solid salt recovery [5, 7, 17]. Furthermore, the consistent linearity enhances confidence in the model's capability to predict salt production and potential revenue from by-product recovery under varying operational capacities.

4.5 Product Water Quality Validation

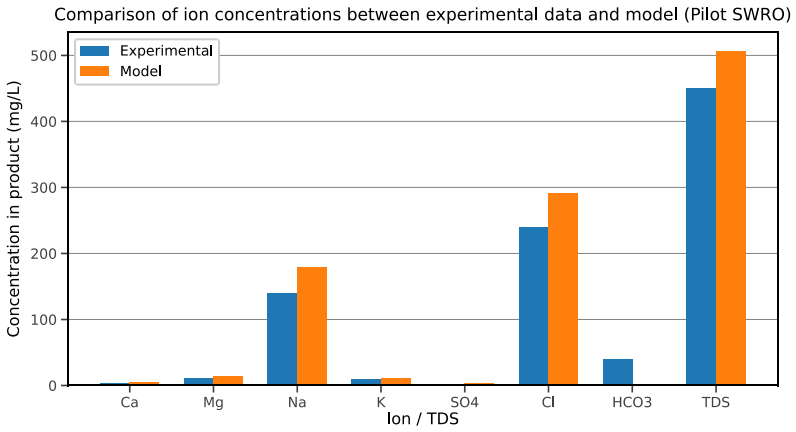


Fig. 14. Comparison of ion concentrations between experimental data and model predictions.

Fig. 14 presents a validation of the predicted product water quality by comparing the concentrations of major ions, including Ca, Mg, Na, K, SO_4, Cl, and HCO_3, as well as the total dissolved solids (TDS) in the final treated water. The figure compares the experimental data from this study (blue bars) with the model predictions reported by Altaee et al. [27] (orange bars). The results indicate that the model slightly overestimates the concentration of most ions in the product water relative to the experimental measurements. This overprediction is particularly evident for sodium, chloride, and TDS. For instance, the model predicts a TDS concentration slightly above 500 mg/L, whereas the experimental data indicate a value close to 450 mg/L. This conservative trend suggests either a cautious membrane transport formulation or a minor underestimation of the effective rejection rates in the RO or AGMD units.

Despite these deviations, the model accurately reproduces the relative rejection behavior of the different ions and provides a reliable estimate of the final water quality. The predicted TDS levels remain well below commonly accepted international drinking water limits, typically 500 mg/L and, in some guidelines, up to 1000 mg/L. These results confirm the suitability of the developed model for predicting product water quality in hybrid desalination systems.

A quantitative assessment of the simplifying assumptions indicates that approximating the feed stream as an equivalent NaCl solution introduces minor deviations that do not undermine overall predictive capability. As demonstrated in Fig. 14, the comparison between the predicted and experimental ion concentrations indicates that the final permeate TDS remains comfortably within potable standards (< 500 mg/L). Furthermore, historical baseline surveys indicate that open-sea salinity remains exceptionally stable over multi-year operational cycles (varying insignificantly over 4-year observation periods); thus, fluctuations in intake composition exert negligible impact on long-term salt recovery rates and final product water quality.

ARTICLE IN PRESS

4.6 Discussion

The coupled RO–AGMD–Spray Dryer system consistently outperforms standalone RO, confirming that integrating AGMD and ZLD processes leads to higher overall freshwater yield. Although the total electrical energy demand is higher, the incorporation of solar thermal energy in the AGMD stage reduces specific energy consumption, enhancing energy efficiency per unit of water produced. Full recovery of brine as solid salt demonstrates the feasibility of zero liquid discharge, mitigating environmental risks associated with conventional brine disposal. The close agreement of modeled water flux, ion concentrations, and salt production with reference data validates the thermodynamic and system-level modeling approach. Moreover, the linear scaling of freshwater and salt output with feed flow allows predictable performance and facilitates operational planning for varying capacities. Nevertheless, assumptions such as constant membrane parameters, simplified brine composition, and idealized spray dryer operation limit precision. Future work should incorporate dynamic modeling, non-linear scaling, multi-ion transport, and detailed thermal modeling of the spray dryer to improve predictive accuracy.

5 Conclusions

This study developed a thermodynamic modeling framework for a solar-driven hybrid desalination system integrating reverse osmosis (RO), air gap membrane distillation (AGMD), and a spray dryer to achieve zero liquid discharge (ZLD) with simultaneous salt recovery. The proposed configuration combines pressure-driven and thermally driven processes, utilizing solar thermal energy from a parabolic trough collector (PTC) to enhance overall system performance and sustainability.

The results demonstrate that the hybrid system significantly increases freshwater production compared to a standalone RO configuration by further recovering water from the RO brine stream through the AGMD unit. At the evaluated operating conditions, the total freshwater output shows a substantial improvement, while the use of solar thermal energy enables partial decoupling of water production from electrical energy demand. Although the total electrical energy consumption increases due to additional system components, the overall performance is improved when assessed in terms of water recovery and potential reduction in specific electrical energy consumption.

The integration of a spray dryer enables complete elimination of liquid brine, achieving zero liquid discharge and allowing recovery of dissolved salts in solid form. The predicted linear relationship between feed flow rate and salt production confirms the consistency of the mass balance and the scalability of the system. In addition, the model indicates that the final product water quality meets typical drinking water standards, supporting the feasibility of the proposed configuration for potable water production.

Despite these promising outcomes, the study relies on several simplifying assumptions, including steady-state operation, simplified brine composition, and system-level modeling of AGMD and spray drying processes. These assumptions may limit the accuracy of the predictions under real operating conditions. Future work should focus on incorporating detailed heat and mass transfer modeling, dynamic system behavior, multi-component salt effects, and experimental validation to improve model reliability and support practical implementation.

Overall, the proposed hybrid RO–AGMD–spray dryer system offers a promising approach for enhancing water recovery, minimizing environmental impacts associated with brine discharge, and utilizing renewable energy in desalination applications, particularly in arid and semi-arid regions with high solar potential.

ARTICLE IN PRESS

Nomenclature

Table 1. List of General Abbreviations and Model Subscripts

Abbreviation	Description
AGMD	Air Gap Membrane Distillation
MED	Multi-Effect Distillation
MSF	Multi-Stage Flash
MD	Membrane Distillation
PTC	Parabolic Trough Collector
PV	Photovoltaic
RO	Reverse Osmosis
SEC	Specific Energy Consumption
TDS	Total Dissolved Solids
ZLD	Zero Liquid Discharge

Subscript	Meaning
f	Feed
p	Permeate
b	Brine
RO	Reverse Osmosis
AGMD	Air Gap Membrane Distillation
SD	Spray Dryer
ZLD	Zero Liquid Discharge
el	Electrical
th	Thermal

Table 2. Symbols for physical parameters, performance indicators, and units

Symbol	Description	Unit
A	Membrane effective area	m^2
Ac	Aperture area of parabolic trough collector	m^2
Cf	Feed water salt concentration	mg/L
Cp	Permeate salt concentration	mg/L
Cb	Brine salt concentration	mg/L
$\dot{m}$	Mass flow rate	kg/s
$\dot{V}$	Volumetric flow rate	m^3/h
F	Feed flow rate	L/h
Jw	Water flux	$kg/m^2 \cdot h$
P	Pressure	bar
ΔP	Transmembrane pressure difference	bar
Q	Heat transfer rate	kW
$Qsolar$	Solar thermal energy input	kW
R	Salt rejection	%
RR	Water recovery ratio	-
SEC	Specific energy consumption	kWh/m^3
T	Temperature	°C
TDS	Total dissolved solids	mg/L
Wel	Electrical power consumption	kW
$\dot{m}salt$	Solid salt production rate	kg/h
η	Efficiency	-
δ	Membrane thickness	m
λ	Thermal conductivity	W/m·K
μ	Dynamic viscosity	Pa·s
ρ	Density	kg/m^3
π	Osmotic pressure	bar

ARTICLE IN PRESS

References

[1] Tarif, A., Kim, B.J., Han, D.S., Park, H., 2025. Solar desalination: current technological status and future directions. Advances in Industrial and Engineering Chemistry, 1(1), 1–17. https://doi.org/10.1007/s44405-025-00027-8

[2] Oraby, H., Ezz, A.A., Hegazy, G.E., 2025. Advances in desalination: pioneering methods and the future of water sustainability. Discover Water, 5(1), 88. https://doi.org/10.1007/s43832-025-00222-0

[3] Essa, M.E.M., El-sayed, H.S., El-kholy, E.E., Amer, M., Elsisi, M., Sajjad, U., Hamid, K., Awad, H.E., 2025. Developments in solar-driven desalination: Technologies, photovoltaic integration, and processes. Energy Conversion and Management: X, 25, 100861. https://doi.org/10.1016/j.ecmx.2024.100861
[4] Wang, W., Aleid, S., Shi, Y., Zhang, C., Li, R., Wu, M., Zhuo, S., Wang, P., 2021. Integrated solar-driven PV cooling and seawater desalination with zero liquid discharge. Joule, 5(7), 1873–1887. https://doi.org/10.1016/j.joule.2021.05.010
[5] Gadalla, M.A., Abdel Fatah, A., Elazab, H.A., 2023. A novel renewable energy powered zero liquid discharge scheme for RO desalination applications. Case Studies in Chemical and Environmental Engineering, 8, 100407. https://doi.org/10.1016/j.cscee.2023.100407
[6] Menon, A.K., Jia, M., Kaur, S., Dames, C., Prasher, R.S., 2023. Distributed desalination using solar energy: A technoeconomic framework to decarbonize nontraditional water treatment. iScience, 26(2), 105966. https://doi.org/10.1016/j.isci.2023.105966
[7] Shi, Y., Zhang, C., Li, R., Zhuo, S., Jin, Y., Shi, L., Hong, S., Chang, J., Ong, C., Wang, P., 2018. Solar Evaporator with Controlled Salt Precipitation for Zero Liquid Discharge Desalination. Environmental Science & Technology, 52(20), 11822–11830. https://doi.org/10.1021/acs.est.8b03300
[8] Sharqawy, M.H., Lienhard, J.H., Zubair, S.M., 2010. Thermophysical properties of seawater: a review of existing correlations and data. Desalination and Water Treatment, 16(1-3), 354–380. https://doi.org/10.5004/dwt.2010.1079
[9] Al-Ghamdi, A.S., Mahmoud, A.M., Bamardouf, K., 2022. Solar desalination methods and economics (literature review). American Journal of Energy Engineering, 10(4), 92–102. https://doi.org/10.11648/j.ajee.20221004.12
[10] Chen, F., Ma, L., Zhang, Z., Wang, X., Wang, Q., Wang, X., Chen, C., Jiang, L., Li, X., 2024. Pilot-scale evaluation of the sustainability of membrane desalination systems for the concentrate volume minimization of coal chemical wastewater. Environmental Science: Water Research & Technology, 10(1), 205–215. https://doi.org/10.1039/d3ew00476g
[11] Prado de Nicolás, A., Molina-García, Á., García-Bermejo, J.T., Vera-García, F., 2023. Desalination, minimal and zero liquid discharge powered by renewable energy sources: Current status and future perspectives. Renewable and Sustainable Energy Reviews, 187, 113733. https://doi.org/10.1016/j.rser.2023.113733
[12] Chen, Q., Burhan, M., Shahzad, M.W., Ybyraiymkul, D., Akhtar, F.H., Li, Y., Ng, K.C., 2021. A zero liquid discharge system integrating multi-effect distillation and evaporative crystallization for desalination brine treatment. Desalination, 502, 114928. https://doi.org/10.1016/j.desal.2020.114928
[13] Zarei, T., Miroliaei, M.R., 2022. Performance evaluation of an HDH desalination system using direct contact packed towers: experimental and mathematical modeling study. Journal of Water Reuse and Desalination, 12(1), 92–110. https://doi.org/10.2166/wrd.2022.095
[14] Nayal, M., Sharma, A.K., Jain, S., Singh, V.P., 2024. Optimization techniques of solar thermal and hybrid energy systems, In: Highly Efficient Thermal Renewable Energy Systems, CRC Press, 104–120. https://doi.org/10.1201/9781003472629-7
[15] Atia, A.A., Yip, N.Y., Fthenakis, V., 2021. Pathways for minimal and zero liquid discharge with enhanced reverse osmosis technologies: Module-scale modeling and techno-economic assessment. Desalination, 509, 115069. https://doi.org/10.1016/j.desal.2021.115069
[16] Fares, M.M., Ju, X., Elgendy, E., Fatouh, M., Zhang, H., Xu, C., Abd El-Samie, M.M., 2024. Techno-exergy-economic assessment of humidification-dehumidification/reverse osmosis hybrid desalination system integrated with concentrated photovoltaic/thermal. Renewable Energy, 227, 120497. https://doi.org/10.1016/j.renene.2024.120497
[17] Al-Sulaiman, F.A., Zubair, M.I., Atif, M., Gandhidasan, P., Al-Dini, S.A., Antar, M.A., 2015. Humidification dehumidification desalination system using parabolic trough solar air collector. Applied Thermal Engineering, 75, 809–816. https://doi.org/10.1016/j.applthermaleng.2014.10.072
[18] Caceres Gonzalez, R.A., Hatzell, M.C., 2024. Electrified Solar Zero Liquid Discharge: Exploring the Potential of PV-ZLD in the US. Environmental Science & Technology, 58(35), 15562–15574. https://doi.org/10.1021/acs.est.4c00494
[19] Al-Obaidani, S., Curcio, E., Macedonio, F., Di Profio, G., Al-Hinai, H., Drioli, E., 2008. Potential of membrane distillation in seawater desalination: Thermal efficiency, sensitivity study and cost estimation. Journal of Membrane Science, 323(1), 85–98. https://doi.org/10.1016/j.memsci.2008.06.006
[20] Zhang, H., Xian, H., 2024. Review of Hybrid Membrane Distillation Systems. Membranes, 14(1), 25. https://doi.org/10.3390/membranes14010025
[21] Fernandez, G.T., He, Z., Kessie, J., Yu, J., 2025. Zero Liquid Discharge of High-Salinity Produced Water via Integrated Membrane Distillation and Crystallization: Experimental Study and Techno-Economic Analysis. Membranes, 15(9), 281. https://doi.org/10.3390/membranes15090281
[22] Alghassab, M.A., 2024. A review of hybrid solar desalination systems: structure and performance. Water Science and Technology, 89(5), 1357–1381. https://doi.org/10.2166/wst.2024.042
[23] Zuo, J., Chow, C.A., Dumee, L.F., Prince, A.J., 2022. A Zero-Brine Discharge Seawater Desalination Using a Pilot-Scale Membrane Distillation System Integrated with Crystallizer. Membranes, 12(8), 799. https://doi.org/10.3390/membranes12080799
[24] Harby, K., Emad, M., Benghanem, M., Abolibda, T.Z., Almohammadi, K., Aljabri, A., Alsaiari, A., Elgendi, M., 2024. Reverse osmosis hybridization with other desalination techniques: An overview and opportunities. Desalination, 581, 117600. https://doi.org/10.1016/j.desal.2024.117600
[25] Wang, Z., Deshmukh, A., Du, Y., Elimelech, M., 2020. Minimal and zero liquid discharge with reverse osmosis using low-salt-rejection membranes. Water Research, 170, 115317. https://doi.org/10.1016/j.watres.2019.115317
[26] Hamawand, I., Lewis, L., Ghaffour, N., Bundschuh, J., 2017. Desalination of salty water using vacuum spray dryer driven by solar energy. Desalination, 404, 182–191. https://doi.org/10.1016/j.desal.2016.11.015

ARTICLE IN PRESS

[27] Altaee, A., 2012. A Computational Model to Estimate the Performance of 8 Inches RO Membranes in Pressure Vessel. Journal of Membrane and Separation Technology, 1(1), 60–71. https://doi.org/10.6000/1929-6037.2012.01.01.8
[28] Winter, D., 2015. Membrane distillation: a thermodynamic, technological and economic analysis, Aachen: Shaker Verlag. https://doi.org/10.2370/9783844037067
[29] McKinney, W., 2010. Data structures for statistical computing in Python. Proceedings of the 9th Python in Science Conference, Austin, Texas, 56–61. https://doi.org/10.25080/Majora-92bf1922-00a
[30] Harris, C.R., Millman, K.J., van der Walt, S.J., Gommers, R., Virtanen, P., Cournapeau, D., Wieser, E., Taylor, J., Berg, S., Smith, N.J., Kern, R., Picus, M., Hoyer, S., van Kerkwijk, M.H., Brett, M., Haldane, A., Fernández del Río, J., Wiebe, M., Peterson, P., Gérard-Marchant, P., Sheppard, K., Reddy, T., Weckesser, W., Abbasi, H., Gohlke, C., Oliphant, T.E., 2020. Array programming with NumPy. Nature, 585(7825), 357–362. https://doi.org/10.1038/s41586-020-2649-2
[31] Hunter, J.D., 2007. Matplotlib: A 2D Graphics Environment. Computing in Science & Engineering, 9(3), 90–95. https://doi.org/10.1109/mcse.2007.55
[32] Ababneh, A.K., Jawarneh, A.M., Tarawneh, M.A., Tlilan, H., Duić, N., 2016. Evaluation of Solar Parabolic Trough Collector for the Application of Seawater Desalination. International Review of Mechanical Engineering, 10(6), 443–451. https://doi.org/10.15866/ireme.v10i6.9480
[33] Khalifa, A., Lawal, D., Antar, M., Khayet, M., 2015. Experimental and theoretical investigation on water desalination using air gap membrane distillation. Desalination, 376, 94–108. https://doi.org/10.1016/j.desal.2015.08.016
[34] Ansar, A., Ahmad Yahaya, A.N., Kamil, A.A., Sabani, R., Murad, M., Aisyah, S., 2022. A new innovative breakthrough in the production of salt from bittern using a spray dryer. Heliyon, 8(10), e11060. https://doi.org/10.1016/j.heliyon.2022.e11060

ARTICLE IN PRESS